CONTINUOUS CONCRETE BEAMS REINFORCED WITH CFRP BARS

By

A. F. Ashour [1] BSc, MSc, PhD, CEng, MIStructE
M. N. Habeeb[2], BSc, MSc

A.F.Ashour is currently a senior lecturer at the University of Bradford, UK. He obtained his BSc and MSc degrees from Mansoura University, Egypt and his PhD from Cambridge University, UK. His research interests include shear, plasticity and optimisation of reinforced concrete and masonry structures.

M. N. Habeeb is a lecturer at Leeds College of Building, UK. He obtained his BSc from Zigazig University Egypt, and his MSc from Leeds University, UK. He is researching in the concrete structures reinforced with Fibre reinforced polymers.

Keywords: continuous concrete beams, carbon fibre reinforced polymers, Deflection, Crack, Capacity.

[1] Corresponding Author, EDT1, School of Engineering, Design and Technology, University of Bradford, Bradford BD7 1DP, West Yorkshire, UK. The corresponding author, Email.: afashour@bradford.ac.uk, Tel. +44 1274 233870.
[2] Lecturer, Leeds College of Building, North Street, Leeds LS2 7QT, UK, E-mail MHabeeb@lcb.ac.uk.

ABSTRACT

This paper reports the testing of three continuously and two simply supported concrete beams reinforced with carbon fibre reinforced polymer (CFRP) bars. The amount of CFRP reinforcement in beams tested was the main parameter investigated. A continuous concrete beam reinforced with steel bars was also tested for comparison purposes. The ACI 440.1R-06 equations are validated against the beam test results.

Test results show that increasing the CFRP reinforcement ratio of the bottom layer of simply and continuously supported concrete beams is a key factor in enhancing the load capacity and controlling deflection. Continuous concrete beams reinforced with CFRP bars exhibited a remarkable wide crack over the middle support that significantly influenced their behaviour. The load capacity and deflection of CFRP simply supported concrete beams are reasonably predicted using the ACI 440.1R-06 equations. However, the potential capabilities of these equations for predicting the load capacity and deflection of continuous CFRP reinforced concrete beams have been adversely affected by the de-bonding of top CFRP bars from concrete.

INTRODUCTION

Fiber reinforced polymer (FRP) bars are considered as a potential replacement for traditional steel reinforcement in many concrete applications, especially those in a severe environment [1]. Since little is known about the behavior of such composite bars [2], extensive research investigations have been undertaken in order to use these new reinforcements for structural applications. Such applications necessitate either developing a new design code or adopting and modifying the current one to account for the engineering characteristics of FRP materials [3].

The ACI 440 Committee introduced a model established through experimental and analytical principles that could predict the flexural capacity as well as the deflection of concrete members reinforced with FRP bars [4]. The ACI 440 equations are a very important step toward the implementation of FRP composites in civil engineering applications; yet the guidelines could be revised when more data become available [5] to enlighten potential users on the applicability of these equations. In a comprehensive study, Vijay [6] presented a simple mathematical model quoting the ACI 318-99 and ACI-440.1R-01 equations to identify failure modes and to compute the moment capacity of 77 simply supported concrete beams reinforced with glass fiber-reinforced polymer (GFRP) bars, extracted from 14 different experimental investigations. The mathematical model presented in Vijay's study provided excellent correlation with respect to the ultimate moment capacity of GFRP reinforced concrete beam test results. On the other hand, Toutanji [5] confirmed the accuracy of the ACI-440.1R-01 equations in predicting the deflections of GFRP simply supported concrete beams. Generally the research presented in the literature recognized the potential of the ACI-440 equations to predict the moment capacity in addition to deflections of simply supported FRP reinforced concrete beams, particularly GFRP reinforced concrete beams due to the availability of data on such beams. Grace et al. [7] presented test results of continuous T-section concrete beams reinforced with different combinations of FRP and steel bars and stirrups. They concluded that the types of FRP reinforcement and stirrups govern the failure mode, and the crack pattern is dependent mainly on the type of stirrups.

This paper investigates the use of CFRP bars as longitudinal reinforcement for continuous concrete beams. Test results have been compared against those of simply supported beams reinforced with identical CFRP bars and a continuously supported concrete beam reinforced with steel bars having similar tensile strength. The ACI

440.1R-06 equations have been validated against experimental results of the beams tested.

TEST PROGRAMME

Test Specimens and Materials

Three continuously and two simply supported CFRP reinforced concrete beams were tested in flexure. In addition, a continuously supported steel reinforced concrete beam was tested for comparison purposes. All beams were 200 mm in width and 300 mm in depth. The simply supported beams had a span of 2750 mm, whereas the continuously supported beams had two spans, each of 2750 mm as shown in Figs. 1 and 2, respectively.

The CFRP reinforced concrete continuous beams were reinforced in a way to accomplish three possible reinforcement combinations at the top and bottom layers. These combinations were: 2ϕ12mm at the top layer and 2ϕ7.5mm at the bottom layer in beam C-C-3, 2ϕ7.5mm at the top layer and 2ϕ12mm at the bottom layer in beam C-C-4 and 2ϕ12mm at the top as well as the bottom layer in beam C-C-5 as shown in Fig. 2 and Table 1. The steel reinforcement (4 bars of 12mm diameter) of the continuous beam S-C-6 was selected to achieve tensile strength of 240 kN, equivalent to that of CFRP reinforcement (2 bars of 12mm diameter) used at the bottom layer of beams C-C-4 and C-C-5 and top layer of beams C-C-3 and C-C-5. All longitudinal reinforcement details including the reinforcement ratio, ρ_f ($=A_f/bd$, where b is the beam width and d is the beam depth), of all beams tested are presented in Table 1. Steel bars of 8 mm diameter were used as vertical stirrups, spaced at 140 mm for all beams tested in accordance with ACI 318-02 [8] to prevent shear failure mode. Tensile tests of

reinforcing bar specimens were conducted until rupture of the rods. Table 2 details the properties of steel and CFRP reinforcing bars used in the beams tested.

The notation of each beam is based on the type of reinforcement and support system. The first letter in the notation represents the type of reinforcement, ‘C’ for CFRP and ‘S’ for steel reinforcement. The second letter corresponds to the supporting system, either ‘C’ for continuously supported beams or ‘S’ for simply supported beams. The third number gives the beam order.

Sand, gravel coarse aggregate (10mm maximum size), and ordinary Portland cement were used to produce concrete with a target compressive strength of 40 N/mm^2 at 28 days. All test specimens were de-moulded after 24hrs, wet cured and covered with polyethylene sheets until the date of testing. Three cubes (100mm) and cylinders (150mm diameter and 300mm high) were tested immediately after testing of each beam to provide values for cube strength f_{cu} and cylinder compressive strength $f_c^{'}$, respectively. Table 1 details all results that have been collected from testing the concrete control specimens.

Test Procedure

Each continuous test beam comprised two equal spans supported on two roller supports, one at the end and the other at the middle, in addition to a hinge support at the other end of the beam, as shown in Fig. 2. Each span of the continuous beams was loaded at its mid point via a hydraulic ram and an independent steel reaction frame, which was bolted to the laboratory floor. Three load cells were used to measure the reactions at one of the end supports, the middle support and at the main applied load from the hydraulic ram as shown in Fig. 2. The simply supported beams were similarly loaded at mid span and supported on a hinge support at one end and a roller support at

the other end as shown in Fig. 1. Mid-span deflections were measured by positioning linear variable differential transformers (LVDTs) at the two mid-spans of continuous beams and the mid-span of simply supported beams. For quality control purposes, dial gauges were also placed adjacent to each LVDT to manually measure deflections of the beams tested. Additional dial gauges were located at the three supports of continuous beams to assess any settlement that might take place during the loading process, which could affect the mid-span deflection readings and the reaction distribution. Load cells and LVDT readings were registered automatically at each load increment at a rate of 6.2kN, using data logging equipment. Failure of the beams tested was judged to occur when the beam under testing could not uphold any additional applied load. At such stage, the applied load was released and no further data were registered by the data logging equipment.

TEST RESULTS

Crack Propagation and Failure Modes

The first visible cracking load of each beam tested is presented in Table 3. The steel reinforced concrete beam cracked at a later stage in comparison with its similar continuously supported CFRP reinforced concrete beam. For the CFRP continuous beams, the earliest crack initiation, at the mid-span sections, was observed in beam C-C-3 reinforced with the smallest CFRP reinforcement ratio at its bottom layer. Beam C-C-4 reinforced with 2ϕ□7.5mm CFRP bars at the top layer, was the first beam to be cracked over the middle support section among the three CFRP reinforced continuous beams. Beam C-C-5 demonstrated the largest cracking load, at either mid-span or middle support section among the three continuous CFRP reinforced concrete beams.

With the load increase, CFRP reinforced concrete beams gradually developed more vertical cracks accompanied by a little noise without any sign of de-bonding. In addition, crack patterns of CFRP reinforced concrete beams at early stage of loading were similar to those of the steel-reinforced concrete beam, but as loads increased, crack spacing decreased and crack width increased compared with the steel beam. This is mainly attributed to the reported lower bond strength values that FRP bars demonstrate in comparison with steel bars [9, 10, 11, 12, 13], since an adequate bond between reinforcing bars and concrete arrests flexural cracking.

It was also observed that the continuous CFRP reinforced concrete beams rapidly developed a remarkably wide crack over the intermediate support as shown in Fig. 3, indicating bond slip between CFRP bars and concrete. It was accompanied with a loud bang. Belarbi and Wang [13] reported that the bond strength of GFRP bars was about twice as much as that of CFRP bars, which consequently would cause an un-tolerated width of cracks in CFRP reinforced concrete beams at large loads. All beams tested exhibited two different modes of failure as explained below:

- Bar rupture failure mode was demonstrated by all CFRP reinforced concrete beams tested. These beams were reinforced with an under-reinforcement ratio of CFRP bars. Thus, it was expected that the strain in the CFRP reinforcement would reach its ultimate limit, at the failed section, before the full exhaustion of ultimate strain of concrete, which usually results in such failure mode, as shown in Fig. 4 for beams C-S-2 and C-C-5. In continuous CFRP reinforced concrete beams, the bottom CFRP bar ruptured at the mid-span section, while the over support section experienced wide cracks, indicating that bond slip would have occurred as explained above and shown in Fig. 3.
- Conventional ductile flexural failure was shown by the steel reinforced concrete beam S-C-6 as shown in Fig. 5. This was attributed to the under-reinforcement ratio used,

which caused yielding of tensile steel bars, followed by concrete crushing at both middle support and mid-span sections.

Load Capacity

Failure loads $P_{t,exp}$ of the beams tested are presented in Table 3. The simply supported reinforced concrete beam C-S-1 failed at nearly 50% of the total failure load of beams C-C-5 and C-C-4. Similarly beam C-S-2 failed at 43% of the total failure load of beam C-C-3. Such harmony in comparison between the load capacities of the simply and continuously supported CFRP reinforced concrete beams is attributed to the identical CFRP reinforcement at the bottom layer of each compared set of beams. Beams C-C-5 and C-C-4 have tolerated more loads than beam C-C-3 as beam C-C-3 is reinforced with less reinforcement ratio of CFRP bars at the bottom layer. A similar trend has also been illustrated by the higher failure load of beam C-S-1 in comparison with that of beam C-S-2.

Even though the reinforcement ratio of the top CFRP bars used in beam C-C-4 was less than half that used in beam C-C-5, beam C-C-4 resisted a failure load similar to that of beam C-C-5. This would indicate that the CFRP top reinforcement was ineffective in enhancing the beam load carrying capacity, but owing to the previously stated de-bonding issue of the top CFRP reinforcement, this conclusion could be challenged.

Although beam S-C-6 was reinforced with steel bars having similar strength to that used in beam C-C-3, it accomplished the highest load capacity among all the continuous beams tested. The failure load achieved by the continuous CFRP reinforced concrete beams tested could have been much higher and significantly comparable to that of the steel reinforced concrete beam, if it was not arrested by the de-bonding of the top layer reinforcement over the middle support of these beams.

Redistribution of Support Reactions

The reactions recorded at the middle and end supports of each continuous beam tested are presented in Fig. 6. To asses the load redistribution of each beam, the elastic reactions at the middle and end supports, assuming a uniform flexure stiffness 'EI' throughout the entire beam, are also plotted in the same figure. Owing to the ductile behaviour of the steel bars, it was expected that beam S-C-6 would demonstrate distinctive load redistribution in comparison with the CFRP reinforced concrete beams tested. Such anticipation has not been exhibited by beam S-C-6 tested as shown in Fig. 6 due to the following reasons:

- The loading system illustrated in Figure 2 produced a small difference between the moment values at mid-span and middle support sections.
- As the amount of steel reinforcement (4 bars of 12mm diameter) used at the top and bottom layers of the steel reinforced concrete beam tested was the same, strains in the top and bottom bars were similar and consequently, the yielding point for the top and bottom steel reinforcement was near enough to be compatible.

All continuous CFRP reinforced concrete beams tested exhibited a very similar trend of end and middle support reactions. However, they failed at different loads. They also demonstrated similar unremarkable moment redistribution behaviour to beam S-C-6 until a certain load. Beyond that load, the support reaction distribution is suddenly shifted as more loads transferred to the end supports leaving the middle support with less load. This sudden shift could be mainly accredited to the previously mentioned wide cracks over the middle support that eventually changed the reaction system of continuously supported beams to that of simply supported beams. However, there is no

remarkable moment redistribution after the above mentioned loading shift owing to the brittle nature of the CFRP bars as depicted in Fig. 6.

Mid-span Deflection

The experimental mid-span point load against mid-span deflection curves of all beams tested are presented in Fig. 7. Each curve represents the average of two readings of deflection obtained from LVDTs and dial gauges at the mid-span of each beam tested. For continuous beams, recorded mid-span deflections at one side were similar to those at the other side. Therefore only one side mid-span deflections are presented in Fig. 7.

Initially, all beams tested were un-cracked and, therefore, exhibited linear load-deflection behaviour. This is accredited to the linear elastic characteristics of concrete, CFRP bars, as well as steel bars before reaching the yielding point. With the increase of loading, cracking occurred at mid-span of each beam, causing a reduction in stiffness. As the CFRP reinforced concrete beams demonstrated wider crack openings than the steel reinforced concrete beam, they exhibited lower stiffness and consequently higher mid-span deflections, as it could be seen from Fig. 7.

Beam C-C-3 exhibited the highest deflection among all continuous CFRP reinforced concrete beams tested, due to the low stiffness, $E_f A_f$, of its bottom reinforcement in comparison with that of the other two continuous CFRP reinforced concrete beams C-C-4 and C-C-5. The large amount of top layer CFRP reinforcement of beam C-C-5, which was equivalent to more than 2.5 times of that used in beam C-C-4, had a small effect on the reduction of the deflection of this beam in comparison with that of beam C-C-4. Beam C-S-1 deflected less than beam C-S-2 as the bottom CFRP reinforcement used in beam C-S-1 had higher stiffness, $E_f A_f$, than that of the bottom CFRP bars in beam C-S-2.

As expected, the steel reinforced concrete continuous beam S-C-6 exhibited the highest stiffness among all continuous beams tested owing to the higher modulus of elasticity of steel than CFRP reinforcement. In addition, only beam S-C-6 demonstrated ductile behaviour before failure, due to yielding characteristics of steel bars.

COMPARISONS OF TEST RESULTS AND ACI 440 PREDICTIONS

Prediction of Moment and Load Capacities

The ACI 440.1R-06 report, based on the balanced FRP reinforcement ratio ρ_{fb} obtained from Eq. 1 below, predicted the moment capacity M of beams reinforced with FRP bars using Eqs. 2 and 3 when the reinforcement ratio ρ_f is less than ρ_{fb}.

$$\rho_{fb} = 0.85\beta_1 \frac{f_c^{'}}{f_{fu}} \frac{E_f \varepsilon_{cu}}{E_f \varepsilon_{cu} + f_{fu}} \quad (1)$$

$$M = A_f f_{fu} (d - \frac{\beta_1 c_b}{2}) \quad (2)$$

$$c_b = \left(\frac{\varepsilon_{cu}}{\varepsilon_{cu} + \varepsilon_{fu}} \right) d \quad (3)$$

where A_f is the area of FRP reinforcement, b and d are the width and effective depth of FRP reinforced concrete beams, f_{fu} is the ultimate tensile strength of FRP bars, ε_{cu} is the ultimate strain of concrete, ε_{fu} is the rupture strain of FRP bars, E_f is the modulus of elasticity of FRP bars, c_b is the neutral axis depth for balanced failure as defined in Eq. 3 and β_1 is a strength reduction factor taken as 0.85 for concrete strength up to and including 27.6 MPa. For strength above 27.6 MPa, this factor is reduced continuously at a rate of 0.05 per each 6.9 MPa of strength in excess of 27.6 MPa, but is not taken less than 0.65.

Comparisons between the predicted moment capacity using the above equations and experimental failure moment at mid-span and central support sections are presented in Table 3. Experimental failure moments at mid-span and central support sections are calculated from the measured end support reaction and mid-span point load at failure. Table 3 indicates that the ACI 440.1R-06 equations reasonably predicted the moment capacity of mid-span section of the simply supported beam C-S-2 and slightly underestimated that of beam C-S-1. The tensile rupture mode of failure is correctly predicted by the ACI 440.1R-06 method for both simply supported CFRP reinforced concrete beams, C-S-1 and C-S-2. The ACI 440.1R-06 equation also reasonably predicted the moment capacity of mid-span section of the three continuously supported CFRP beams. However, the failure moment at the central support section of the three continuously supported CFRP beams is significantly overestimated by the ACI 440 equations as it is adversely affected by the wide cracks over the central support and debonding of CFRP bars.

The load capacity P of the simply supported CFRP reinforced concrete beams C-S-1 and C-S-2 is estimated by satisfying the equilibrium condition at the mid-span critical section ($P = 4M_{us}/l$, where M_{us} is the mid-span section moment capacity calculated using the ACI 440.1R-06 equations and l is the beam span). Similar to the mid-span moment capacity prediction, the load capacity of the simply supported beam C-S-2 is reasonably predicted and that of beam C-S-1 is slightly underestimated as presented in Table 3.

On the other hand, the continuous steel reinforced concrete beam was under-reinforced and exhibited ductile failure; therefore, the prediction of its flexural load capacity is based on a collapse mechanism with plastic hinges at mid span and central

support sections. Thus, the flexural load capacity P on each span would be calculated from:

$$P = \frac{2}{l}\left(M_{uh} + 2M_{us}\right) \quad (4)$$

where M_{us} and M_{uh} are moment capacities at mid-span and over support sections, respectively, and l is the beam span. The total predicted load capacity P_t (=2P) obtained from Eq. (4) for the continuous steel beam S-C-6 is 350.9 kN; that is reasonably compared with the experimental failure load of 332.3 kN as presented in Table 3. However, the above principle would not be applicable to CFRP continuous beams because of the brittle nature of either concrete crushing or FRP rupture mode of failure. In addition, CFRP continuous beams displayed wide cracks developed over the middle support section (See Fig. 3) due to de-bonding of the top CFRP bars well before failure. Therefore, Eq. (4) can be modified to account for the debonding occurred at the central support as below:

$$P = \frac{2}{l}\left(M_{b} + 2M_{us}\right) \quad (5)$$

where M_b is the debonding moment at the central support. The debonding moment M_b depends on the level of force in CFRP bars at failure and the bond-slip relationship between CFRP bars and concrete. These parameters are not easily available; therefore, the value of debonding moment at failure would be calculated by re-arranging the above equation and using the actual failure load of each CFRP continuous beam as given in Table 3. Comparisons between the calculated debonding moment M_b at failure and central support hogging moment capacity M_{uh} predicted by the ACI 440 equations for the three CFRP continuous beams are presented in Table 3. This comparison shows that debonding moment at failure occurred at around 30-40% of the section moment capacity.

Deflection Prediction

The immediate deflection Δ of simply and continuously supported reinforced concrete beams loaded with a mid-span point load illustrated in Figs. 1 and 2, could be calculated by Eqs. (6) and (7), respectively, given below:

$$\Delta = \frac{Pl^3}{48E_c I_e} \tag{6}$$

$$\Delta = \frac{7}{768}\frac{Pl^3}{E_c I_e} \tag{7}$$

where P is the mid-span applied load at which the deflection is computed, l is the beam span, E_c is the modulus of elasticity of concrete and I_e is the effective moment of inertia of the beam section. A modified expression for the effective moment of inertia, I_e, to be used for predicting the deflection of FRP reinforced concrete beams is proposed by ACI 440 Committee as follows:

$$I_e = \left[\frac{M_{cr}}{M_a}\right]^3 \beta_d I_g + \left[1 - \left[\frac{M_{cr}}{M_a}\right]^3\right] I_{cr} \le I_g \tag{8}$$

where M_{cr} is the cracking moment = $2 f_{cr} I_g / h$, M_a is the applied moment, β_d (≤ 1) is a reduction coefficient = $0.2\rho_f / \rho_{fb}$, I_g is the gross moment of inertia = $bh^3/12$, b and h are the width and overall height of the concrete beam, respectively, I_{cr} is the moment of inertia of transformed cracked section = $\left(bd^3/3\right)k^3 + n_f A_f d^2 (1-k)^2$, k is the ratio of the neutral axis depth to reinforcement depth = $\sqrt{(\rho_f n_f)^2 + 2\rho_f n_f} - \rho_f n_f$, $n_f (=E_f/E_c)$ is the modular ratio between FRP reinforcement and concrete, E_c = $4750\sqrt{f_c'}$ (N/mm^2) and f_{cr} is the modulus of rupture of concrete = $0.62\sqrt{f_c'}$ (N/mm^2).

Comparisons between predicted by ACI 440 and experimental deflections for the two simply supported beams, C-S-1 and C-S-2, are presented in Fig. 8. It shows that the

experimental deflection of the simply supported beams tested compared reasonably with the predicted deflection at early stages of loading. As the load is increased, however, a proportionally stiffer trend is predicted by the ACI 440 equations.

Fig. 9 also shows comparisons between experimental load-deflection curves obtained in this study and those predicted from Eqs. (7) and (8) for continuous CFRP reinforced concrete beams C-C-3 and C-C-5. At early stages, the ACI 440 equations closely predicted the two beam deflections. In addition, the transition stiffness from uncracked to cracked beam is reasonably predicted. But, after the occurrence of wide cracks over the intermediate support, the ACI 440 predictions are very much stiffer. However, Eq. (7) could be modified to accommodate the debonding moment rather than the elastic moment at the central support as below:

$$\Delta = \frac{Pl^3}{48E_c I_e} - \frac{M_b l^2}{16E_c I_e} \qquad (9)$$

The mid-span deflections obtained from Eqs. (8) and (9) are also plotted in Fig. 9 for the two beams C-C-3 and C-C-5. When the debonding moment is considered, a closer mid-span deflection prediction to that from experiments is achieved.

CONCLUSIONS

The above reports on the testing of three continuously and two simply supported concrete beams reinforced with CFRP bars. Test results were compared with the ACI 440 predictions for moment capacity and deflections. The following conclusions are drawn from the study:

- Increasing the CFRP reinforcement of the bottom layer of simply and continuously supported concrete beams is a key factor in enhancing the load capacity and controlling deflection.

- Increasing the top layer CFRP reinforcement of continuous beams slightly reduced deflections, but has not shown any load capacity improvement.
- Load and moment capacities of CFRP simply supported concrete beams is reasonably predicted using ACI 440.1R-06 equations. However, the potential of these equations for predicting the load capacity of continuous CFRP reinforced concrete beams need to be verified against further test results, making an allowance for the bond strength of CFRP bars and concrete.
- The ACI 440.1R-06 equations seem to be effective in predicting the deflection of CFRP simply and continuously supported concrete beams up to the initiation of excessive cracks. Beyond that the prediction process, particularly for the continuously supported CFRP reinforced concrete beams, has been unconstructively affected by the loss of bond between CFRP top reinforcement and concrete.
- In the continuous CFRP reinforced concrete beams, de-bonding of CFRP bars from concrete appears to be an important issue that needs to be further investigated.

REFERENCES

1. Wu, Z.J. and Ye, J.Q., “Strength and fracture resistance of FRP reinforced concrete flexural members”, *Cement and Concrete Composites*, 25, 2, 2003, pp. 253-261.
2. Benmokrane, B., Tighiouart, B.and Theriault, M., “Bond Strength of FRP Rebar Splices. Non-Metallic (FRP) Reinforcement for Concrete Structures”, *Proceedings of the Third International Symposium on Non-metallic (FRP) Reinforcement for Concrete Structures* (FRPRCS-3), 1997, pp. 405-412.
3. Al-Sayed, S.H., AL-Salloum, Y.A. and Almusallam, T. H., “Performance of Fibre reinforced Plastic Bars as a Reinforcing Material for Concrete Structures”, *Composites Part B: Engineering*, 31, 2000, pp. 555-567.

4. ACI440, *Guide for the Design and Construction of Concrete Reinforced with FRP bars.* ACI committee 440, 2001, re-published 2006, 44pp.

5. Toutanji, H.A. and Saafi M., “Flexural behavior of concrete beams reinforced with glass fiber-reinforced polymer (GFRP) bars”, ACI Structural Journal, 97, 5, 2000, pp. 712-719.

6. Vijay, P. and GangaRao, H.V.S., “Bending Behavior and Deformability of Glass Fibre-Reinforced Polymer Reinforced Concrete Members”, ACI Structural Journal, 98, 6, 2001, pp. 834-842.

7. Grace, N.F., et al., “Behavior and ductility of simple and continuous FRP reinforced beams”, *Journal of Composites for Construction*, 2**,** 4, 1998, pp. 186-194.

8. ACI-committee-318, “Building Code Requirements for Structural Concrete (ACI 318-02) and Commentary (ACI 318R-02)”, 2002.

9. Achillides, Z. and Pilakoutas, K., “Bond behavior of fiber reinforced polymer bars under direct pullout conditions”*, Journal of Composites for Construction*, 8, 2, 2004, pp. 173-181.

10. Cosenza, E., Manfredi, G. and Realfonzo, R., “Behavior and modeling of bond of FRP rebars to concrete”, *Journal of Composites for Construction*, 1**,** 2, 1997, pp. 40-51.

11. Okelo, R. and Yuan R.L., “Bond strength of fiber reinforced polymer rebars in normal strength concrete*”, Journal of Composites for Construction*, 9**,** 3, 2005, pp. 203-213.

12. Tighiouart, B., Benmokrane, B. and Gao, D. “Investigation of bond in concrete member with fibre reinforced polymer (FRP) bars”, *Construction and Building Materials*, 12, 8, 1998, pp. 453-462.

13. Belarbi, A., Wang, H., “Bond-Slip Response of FRP Reinforcing Bars in Fiber Reinforced Concrete under Direct Pullout*”, Proceedings of the International Conference*

on Fibre Composites, High-Performance Concretes and Smart Materials, Chennai, India, 2004. pp. 409-419.

14. Portland Cement Association, “Notes on ACI 318-95 Building Code Requirements for Structural Concrete”, 1996, Section 5, 10p.

Table 1 Details of test specimens.

Beam Notation	Total Length (mm)	Top reinforcement			Bottom reinforcement			Concrete strength (MPa)	
		No.	Dia. (mm)	ρ_f%	No.	Dia. (mm)	ρ_f%	$f_c^{'}$	f_{cu}
C-S-1	2750	2 CFRP	12	0.42	2 CFRP	12	0.42	26. 9	31.8
C-S-2	2750	2 CFRP	7.5	0.16	2 CFRP	7.5	0.16	27.5	31.1
C-C-3	5500	2 CFRP	12	0.42	2 CFRP	7.5	0.16	23.6	31.1
C-C-4	5500	2 CFRP	7.5	0.16	2 CFRP	12	0.42	27.2	31.0
C-C-5	5500	2 CFRP	12	0.42	2 CFRP	12	0.42	28.0	31.8
S-C-6	5500	4 Steel	12	0.85	4 Steel	12	0.85	26.3	32.1

Table 2 FRP and steel reinforcement properties.

Type of Bars	Diameter (mm)	Elastic modulus, E_f (GPa)	Ultimate strength, f_{fu} (MPa)	Ultimate strain, ε_{fu}	Yield strength (MPa)
CFRP	7.5	200	2000	0.010	N/A
CFRP	12	200	1061	0.005	N/A
Steel (Stirrups)	8	206.8	611.6	Not measured	525.5
Steel	12	200	594.4	Not measured	510.8

Table 3 Comparisons between experimental and predicted results.

Beam	Experimental data						ACI prediction			$M_{us}/M_{s,exp}$	$M_{uh}/M_{h,exp}$	M_b (kNm)	M_b/M_{uh}
	$P_{cr,s}$ (kN)	$P_{cr,h}$ (kN)	$P_{t,exp}$ (kN)	$M_{s,exp}$ (kNm)	$M_{h,exp}$ (kNm)	Failure mode	M_{us} (kNm)	M_{uh} (kNm)	P_t				
C-S-1	17.3	N/A	93.3	64.11	N/A	CFRP rupture	53.83	N/A	78.30	0.84	N/A	N/A	N/A
C-S-2	15.9	N/A	64.4	44.28	N/A	CFRP rupture	42.23	N/A	61.43	0.95	N/A	N/A	N/A
C-C-3	18.3	18.3	150.5	44.76	13.97	CFRP rupture	53.83	42.24	N/A	1.20	3.02	17.69	0.42
C-C-4	21.2	12.2	187.9	60.66	7.89	CFRP rupture	42.24	53.83	N/A	0.70	6.82	21.51	0.40
C-C-5	22.1	24.9	180.6	56.03	12.10	CFRP rupture	53.87	53.87	N/A	0.96	4.45	16.29	0.30
S-C-6	46.9	46.9	332.3	78.12	72.22	Ductile flexure	76.15	76.15	350.9	0.97	1.05	N/A	N/A

Note: $P_{cr,s}$ and $P_{cr,h}$ = first visual cracking loads at mid-span and over central support, respectively, $P_{t,exp}$ = total experimental failure load, $M_{s,exp}$ and $M_{h,exp}$ = experimental mid-span and over support moments, respectively, M_{us} and M_{uh} = ACI 440 predicted mid-span and over support moment capacities, respectively, P_t = predicted total load capacity, M_d = debonding moment at failure.

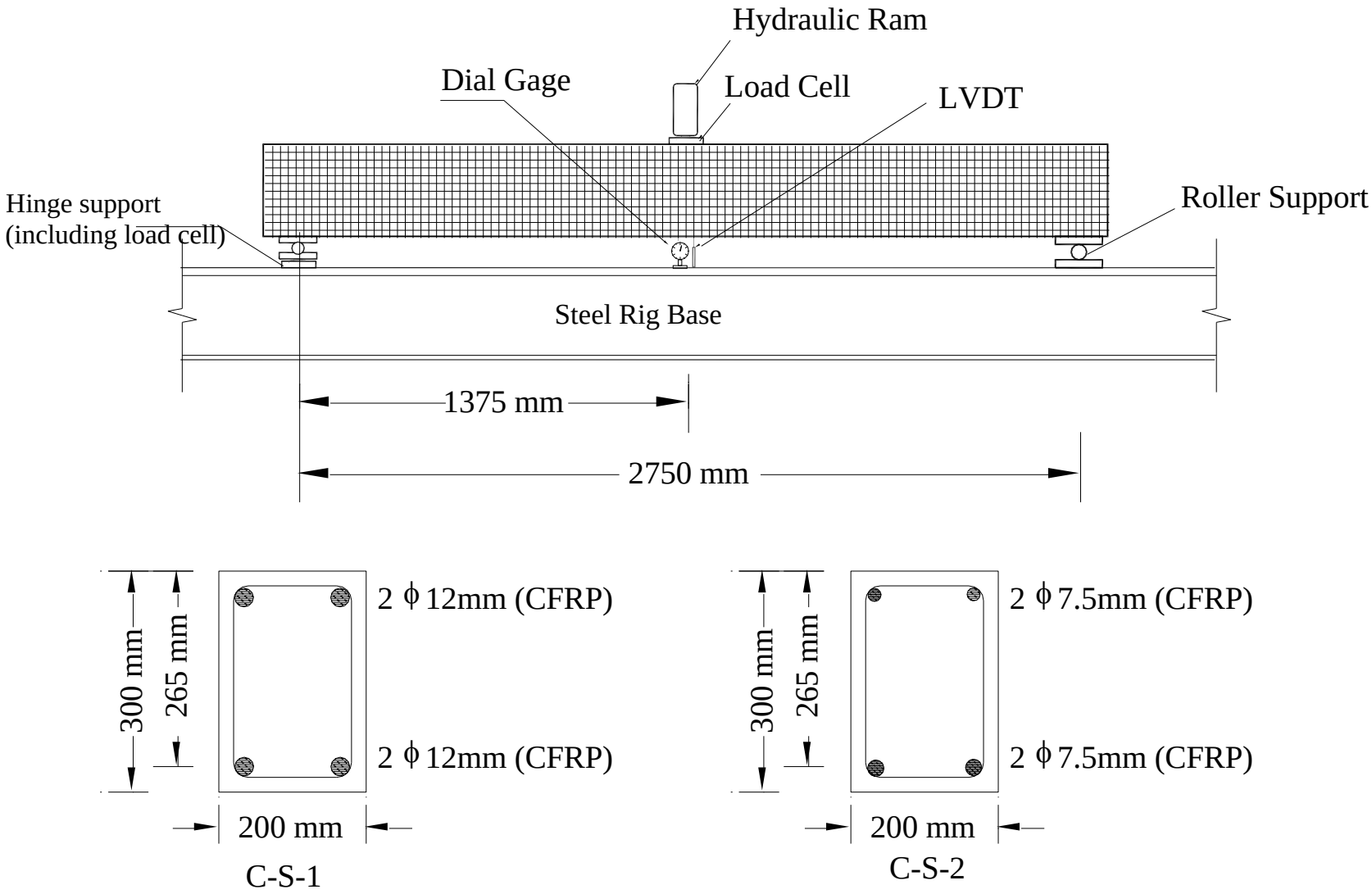

Fig. 1 Test set-up and cross-section details of simply supported beams.

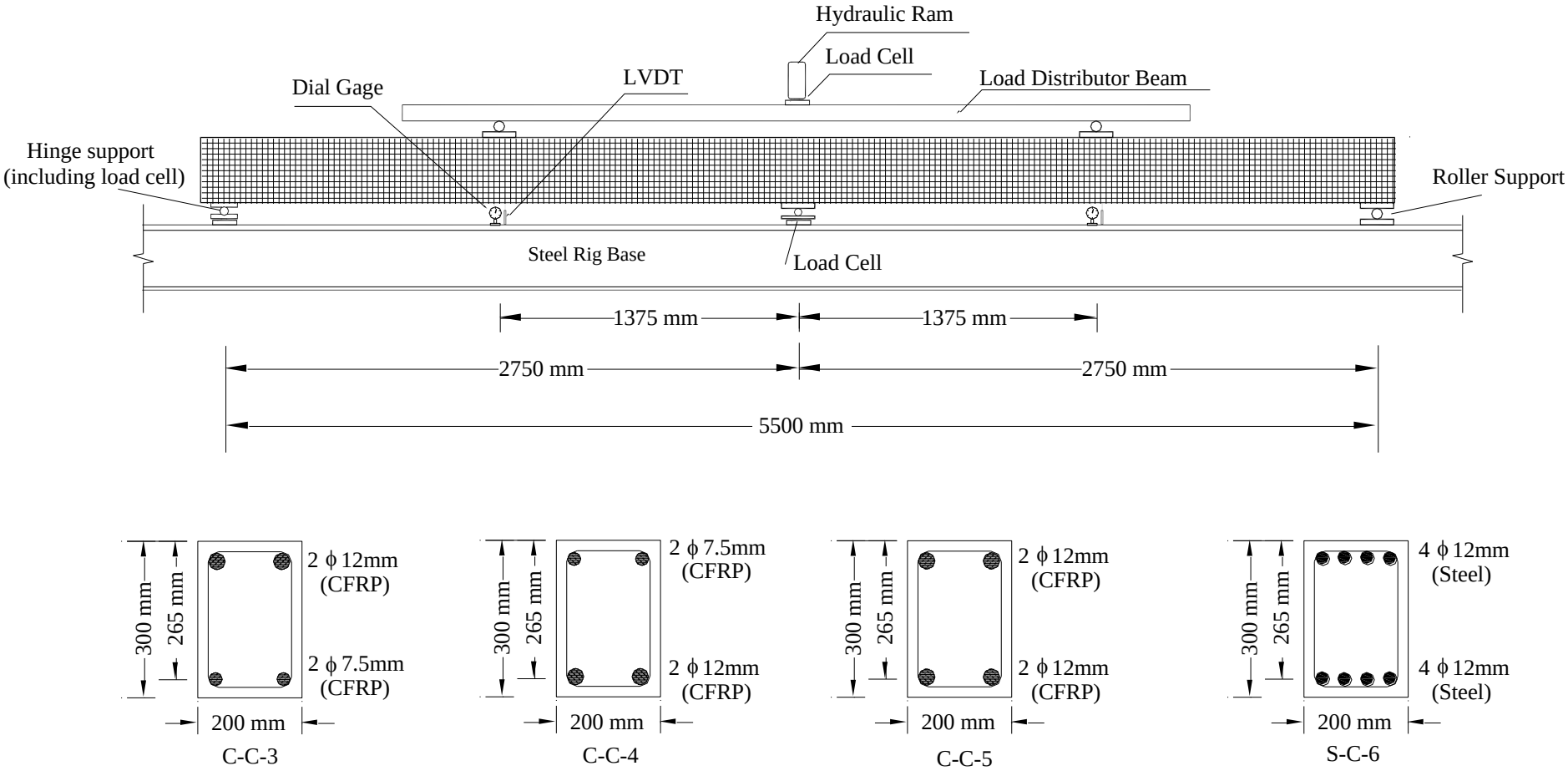

Fig. 2 Test set-up and cross-section details of continuous beams.

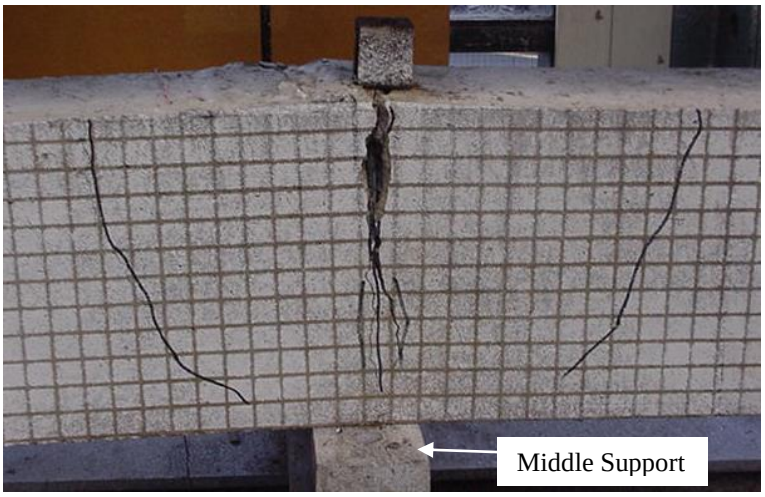

(a) C-C-3

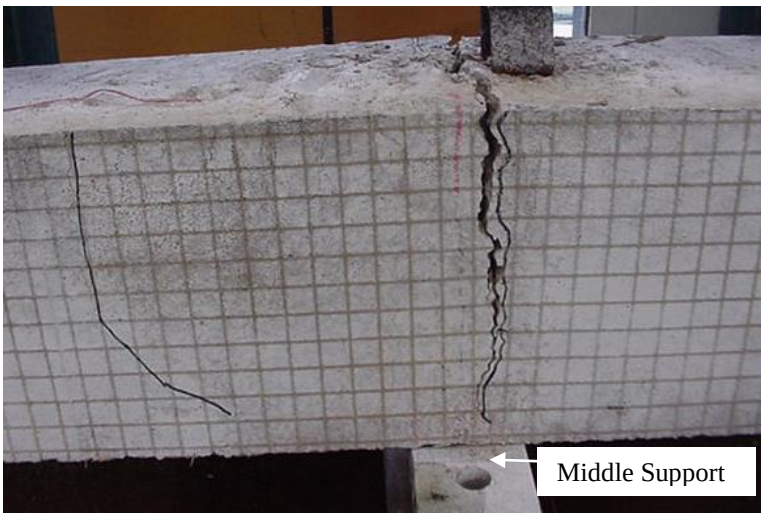

(b) C-C-4

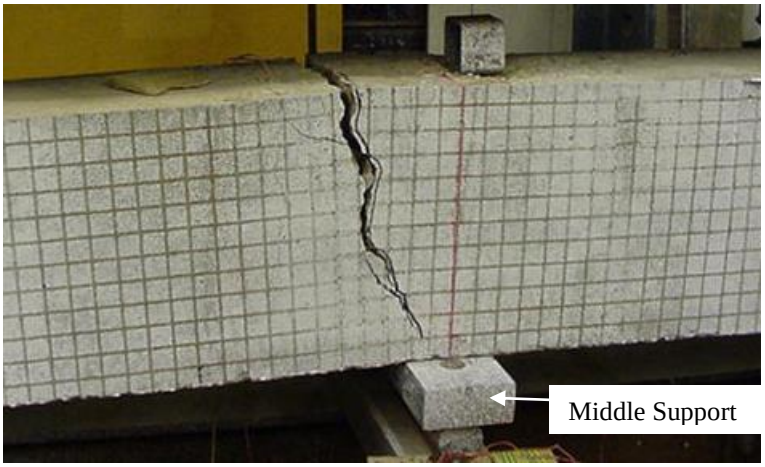

(c) C-C-5

Fig. 3 Wide cracks at the middle support of continuous CFRP reinforced concrete beams tested.

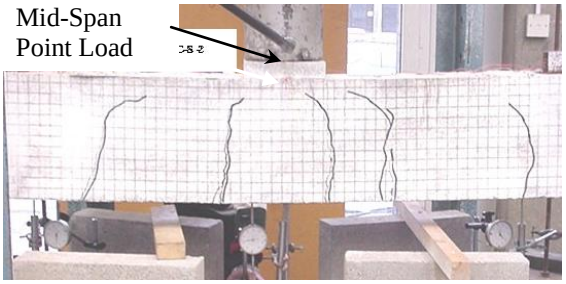

(a) C-S-2

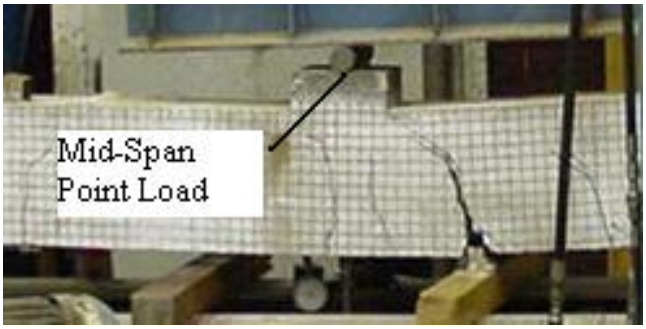

(b) C-C-5

Fig. 4 Bar rupture failure mode of CFRP beams.

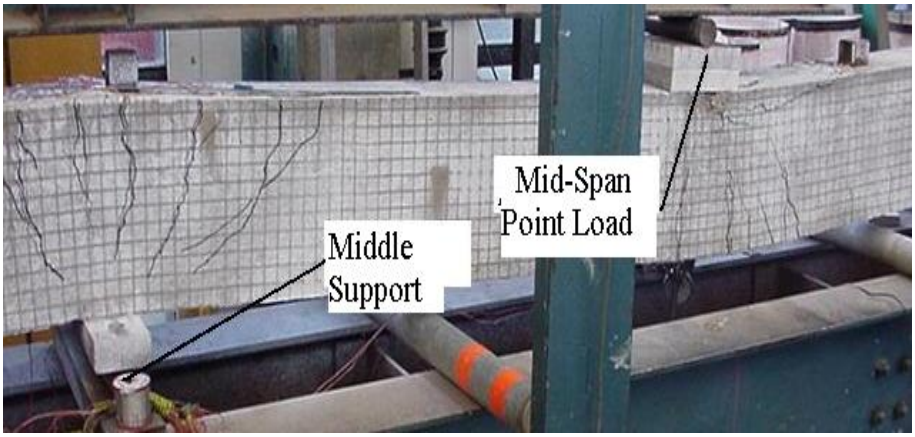

Fig. 5 Conventional ductile flexural failure occurred for beam S-C-6.

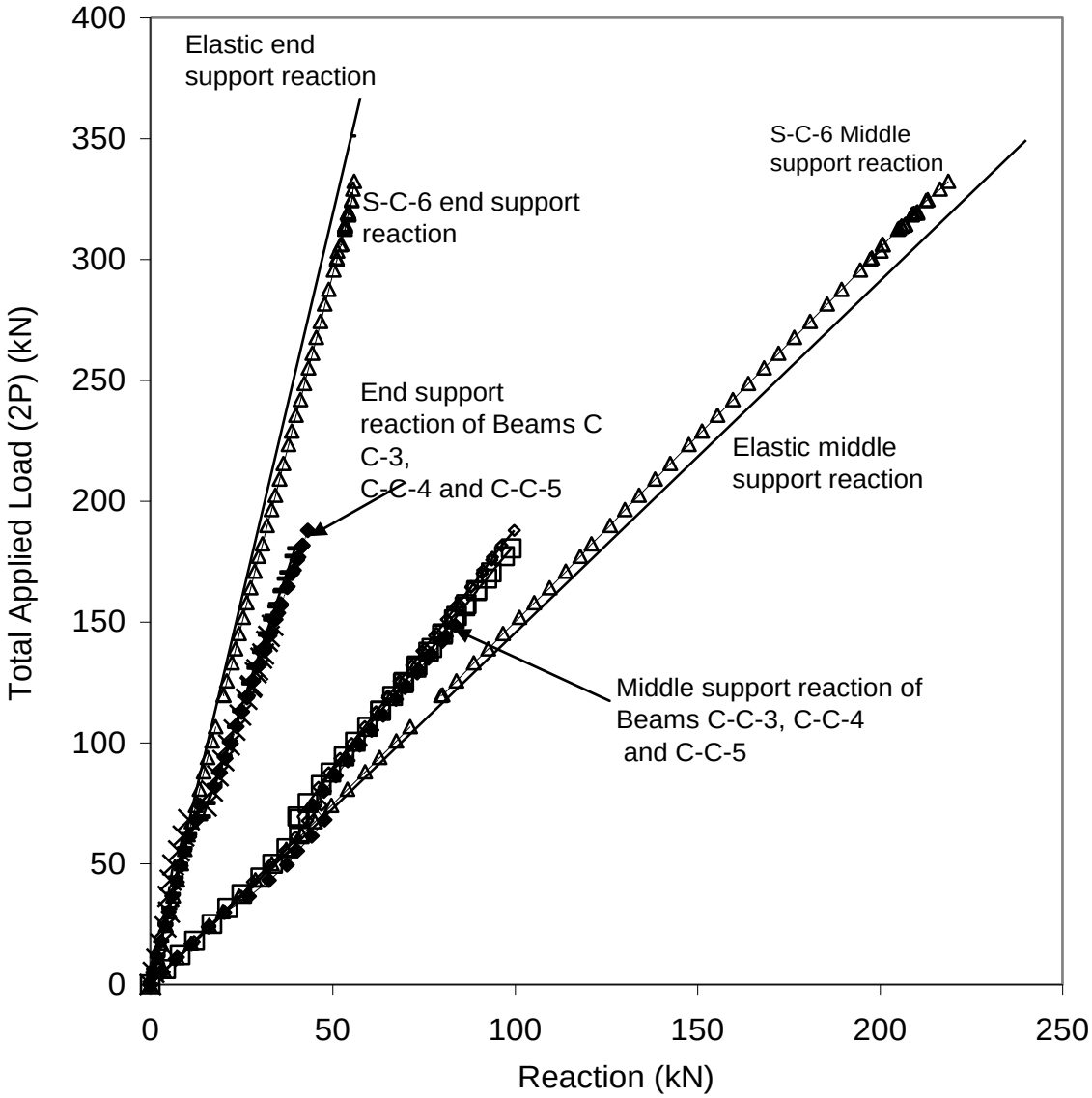

Fig. 6 Support reactions of continuous beams tested

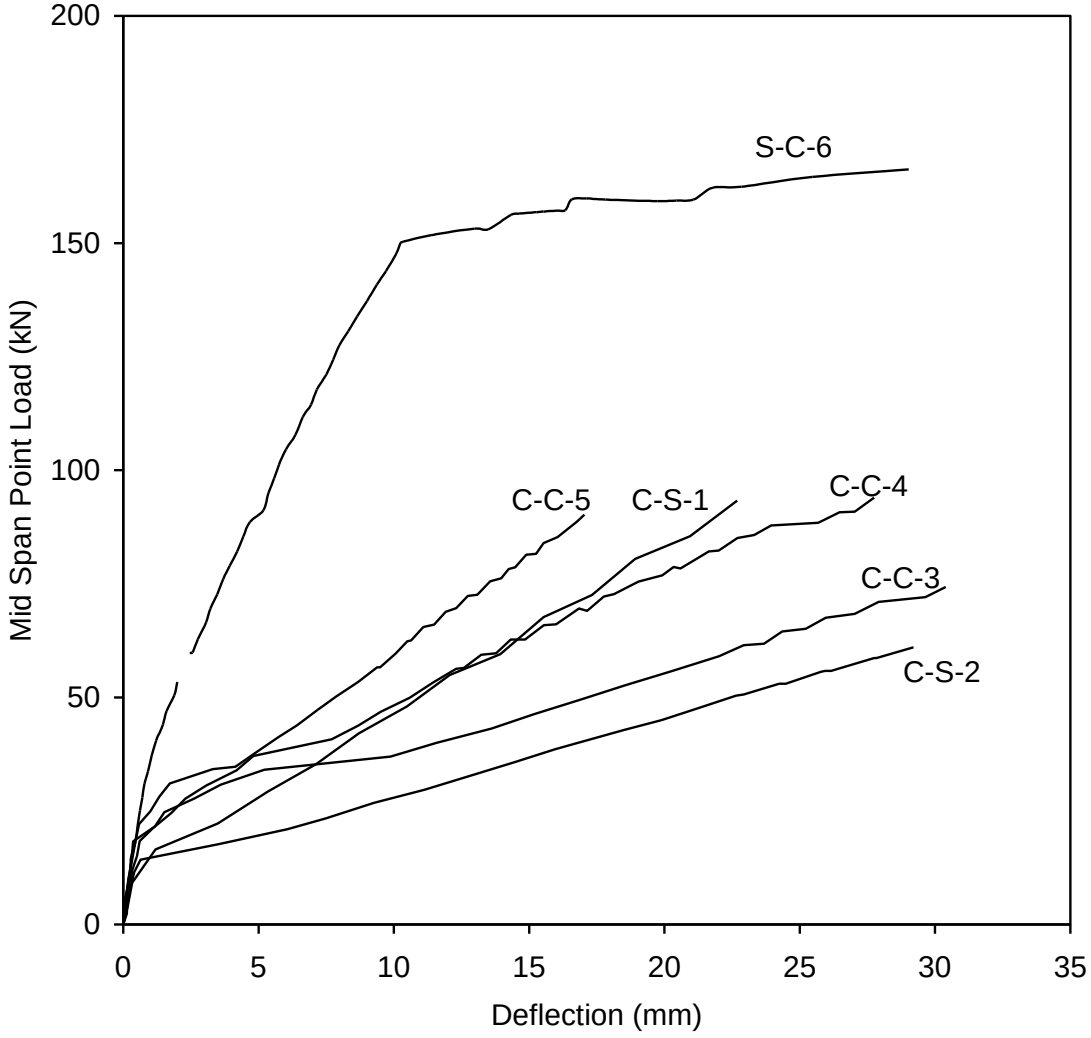

Fig. 7 Experimental mid-span deflections of beams tested.

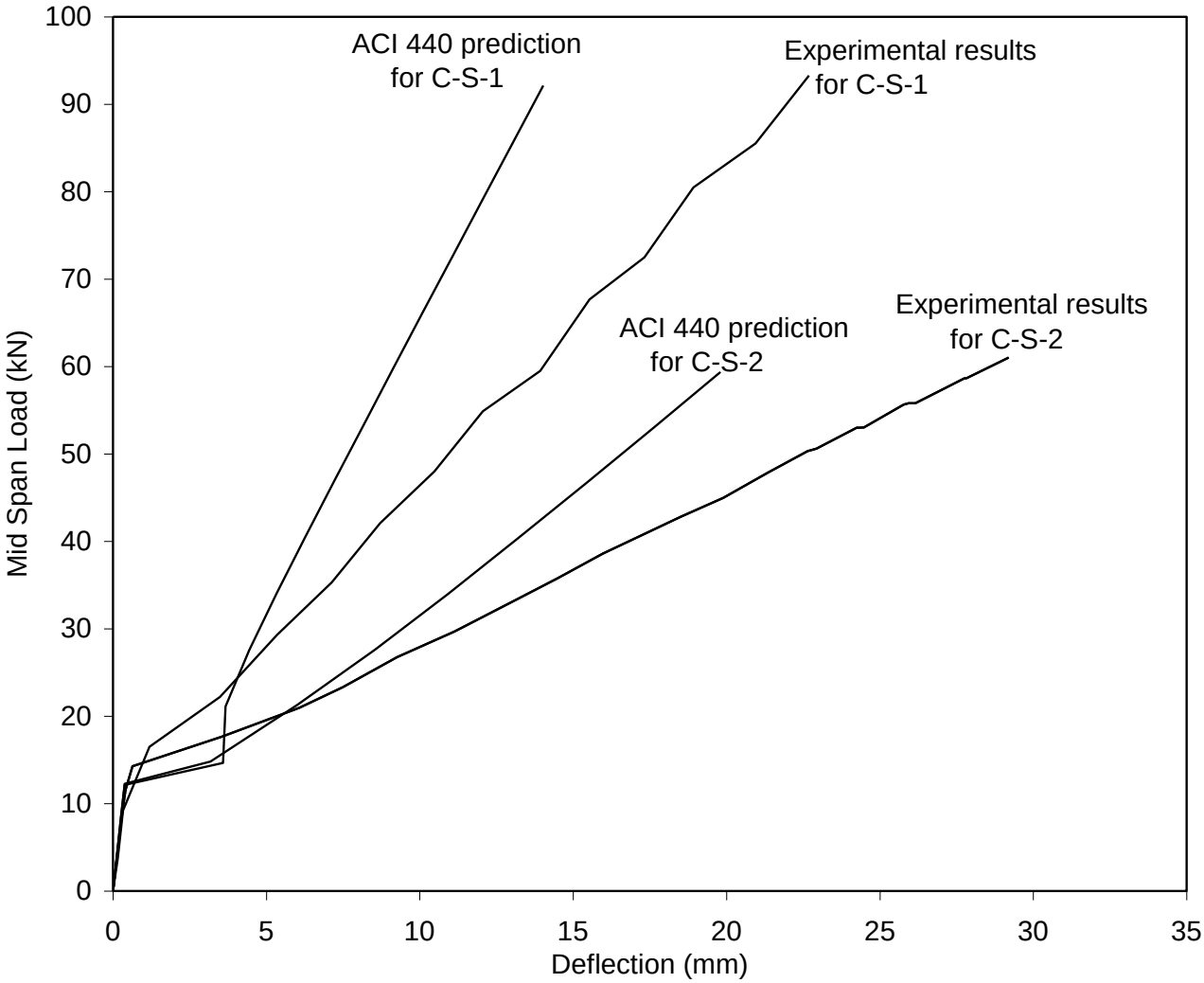

Fig. 8 ACI 440 and experimental deflections of simply supported CFRP reinforced concrete beams tested.

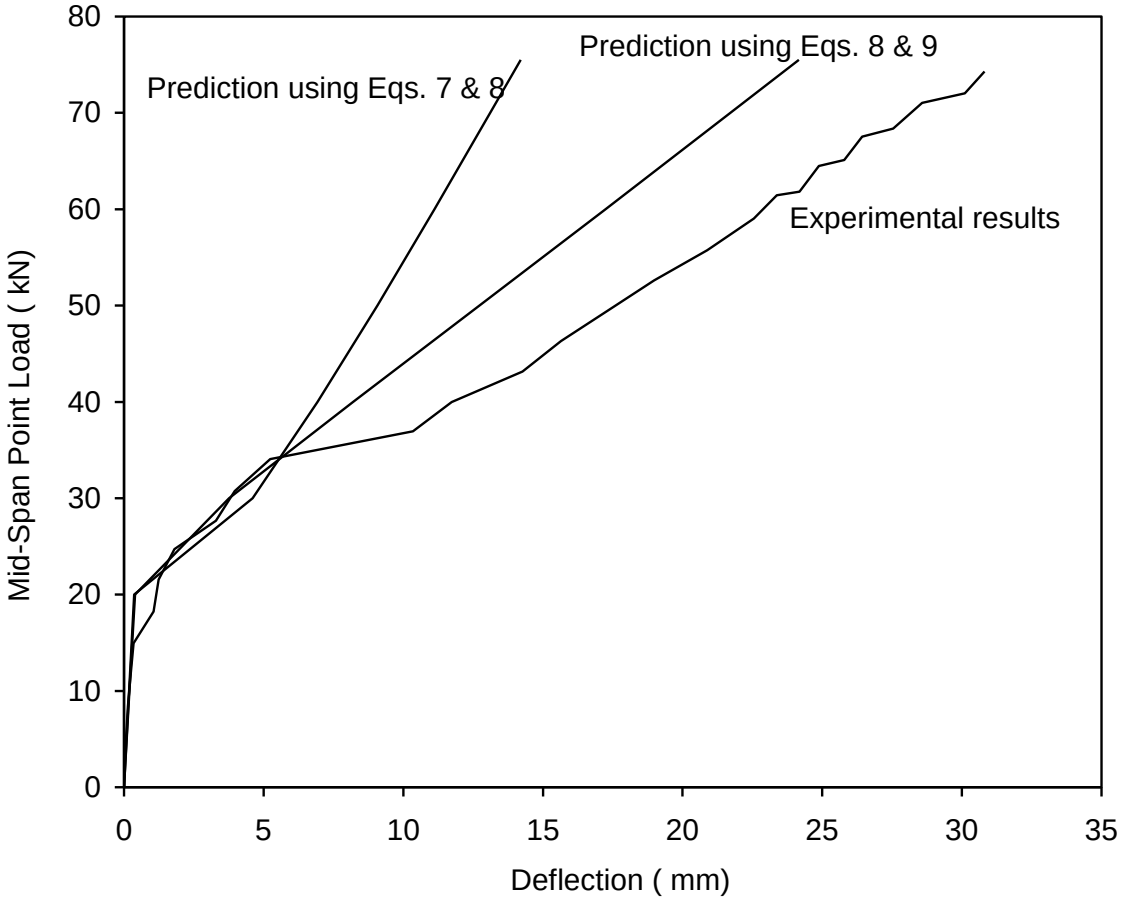
Prediction using Eqs. 8 & 9
Prediction using Eqs. 7 & 8
Experimental results
Mid-Span Point Load (kN)
Deflection (mm)
0
10
20
30
40
50
60
70
80
0
5
10
15
20
25
30
35

(a) C-C-3

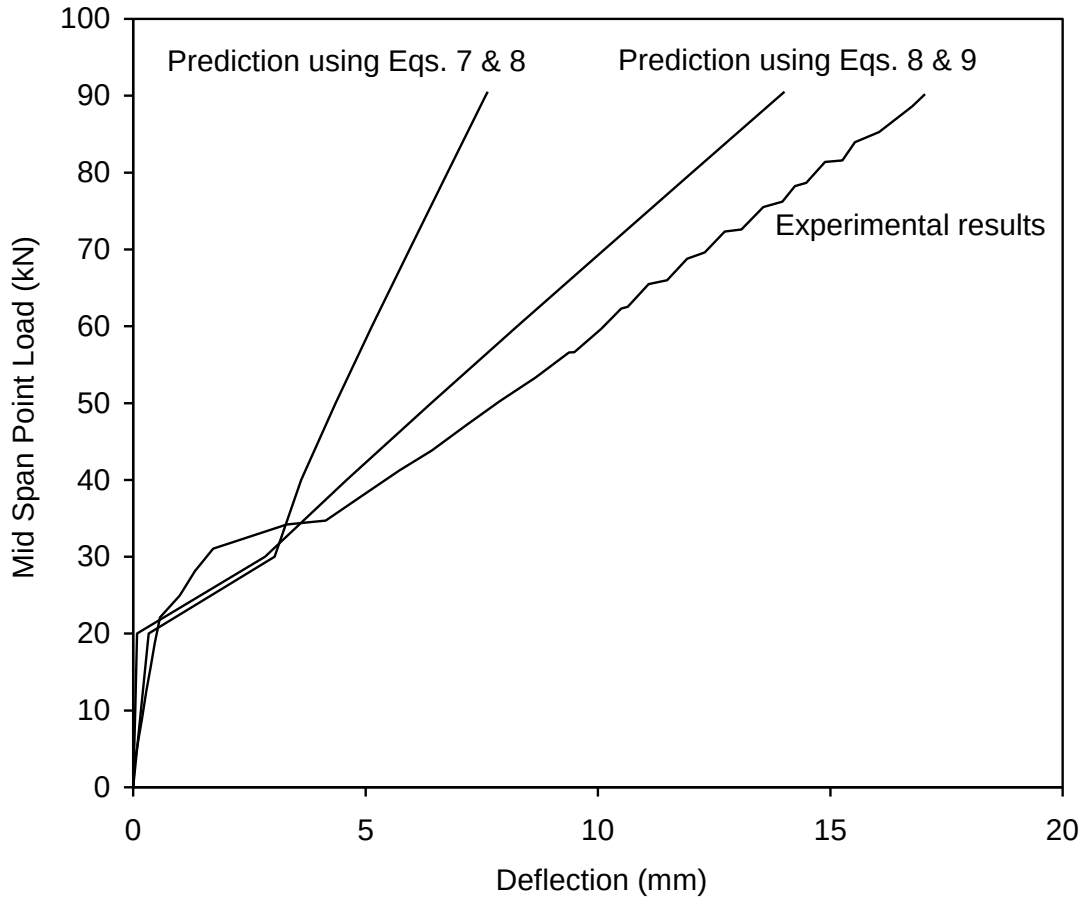

(b) C-C-5

Fig. 9 Comparisons between ACI and experimental deflections of Continuous CFRP reinforced concrete beams.